

Quantum Geometric Planar Magnetotransport: A Probe for Magnetic Geometry in Altermagnets

Zhi-Chun Ouyang,* Wei-Jing Dai,* Zi-Ting Sun,† Jin-Xin Hu,‡ and K. T. Law

Department of Physics, The Hong Kong University of Science and Technology, Clear Water Bay, Hong Kong, China

Nonlinear and nonreciprocal transport phenomena provide a direct probe of band quantum geometry in noncentrosymmetric magnetic materials, such as the nonlinear Hall effect induced by the quantum metric dipole. In altermagnets, a recently discovered class of even-parity collinear magnets with $C_n\mathcal{T}$ symmetry, conventional second-order responses are prohibited by an emergent C_{2z} symmetry. In this work, we demonstrate that an in-plane magnetic field lifts this prohibition, inducing a planar magnetotransport that directly probes the intrinsic quantum geometry and the distinctive $C_n\mathcal{T}$ nature of altermagnetic orders. We show that the field-dependent quantum geometric susceptibility generates versatile planar magnetotransport, including the planar Hall effects and nonreciprocal responses. Our work establishes distinctive signatures of altermagnetism in linear and nonlinear magnetotransport, providing a general framework for measuring quantum geometric responses and probing altermagnetic order.

Introduction. —Nonlinearity and nonreciprocity have been identified as key paradigms for engineering quantum materials and devices [1–9]. Representative examples include the nonlinear Hall effect induced by Berry curvature multipoles in time-reversal-symmetric systems [10–12], nonreciprocal magnetochemical anisotropy [13], and nonlinear optical responses [14], all of which have been extensively investigated in recent years. Recently, the nonlinear Hall effect and nonreciprocal transport were observed in MnBi_2Te_4 , an unconventional \mathcal{PT} -symmetric antiferromagnet [15–19]. Quantum geometry, including the Berry curvature and the quantum metric, has a profound impact on such phenomena, motivating us to explore how transport in unconventional magnets is governed by quantum geometry [20–24].

Growing interest surrounds altermagnets, a class of collinear antiferromagnets with weak spin-orbit coupling (SOC) that share features of both ferromagnets and anti-ferromagnets [25, 26]. Their most prominent property is an even-parity spin splitting in momentum space, which occurs despite a zero net magnetization. Unlike conventional antiferromagnets, where two magnetic sublattices are related by translation or inversion, in altermagnets they are related by a spin-group operation—a combination of a spin flip and a C_n spatial rotation. This description, however, strictly holds only for vanishing SOC; when SOC is present, the spin group reduces to a $C_n\mathcal{T}$ magnetic group [26, 27]. Furthermore, weak SOC is crucial for observing various phenomena in altermagnets [26], such as the anomalous Hall effect [28]. Nevertheless, due to the constraint of an emergent C_{2z} symmetry, second-order transport is prohibited in these systems [29, 30].

Therefore, two fundamental challenges remain. First, how can electronic transport probe the magnetic geometry, i.e., the $C_n\mathcal{T}$ symmetry of altermagnetic spin textures [31]? Second, given that the C_{2z} is preserved in altermagnets, intrinsic second-order nonlinear transport is forbidden. How, then, can we access intrinsic second-

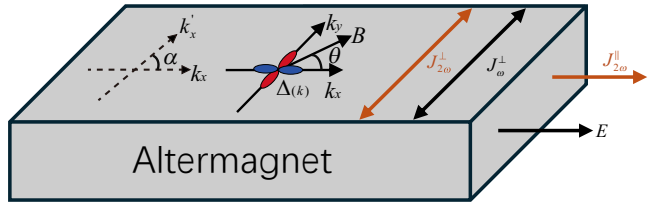


FIG. 1. The schematic picture of the planar magnetotransport of the altermagnets with $C_n\mathcal{T}$ symmetry. Coupled with the in-plane magnetic field, the C_{2z} is broken, resulting in the linear planar Hall effect J_ω^\perp , the nonlinear second-order planar Hall effect $J_{2\omega}^\perp$, and nonreciprocal transport $J_{2\omega}^\parallel$. θ and α label the angle between B field and E field, and the orientation of the sample with respect to E field.

order responses in these systems to directly probe their quantum geometry?

In this work, we propose using an in-plane magnetic field as a powerful probe of the magnetic geometry of altermagnets. As noted above, the altermagnetic order in two dimensions exhibits $C_n\mathcal{T}$ symmetry. We therefore apply an in-plane field B and, for clarity, consider only its Zeeman coupling to spin. This coupling induces finite conductivity responses. Simultaneously, the in-plane field breaks the mirror and C_{2z} symmetries of the altermagnet, thereby enabling both the linear Hall effect and second-order nonlinear transport.

To be concrete, we explicitly show that the quantum-geometric susceptibility with respect to the magnetic field leads to two key transport phenomena: the nonreciprocal longitudinal conductivity and the intrinsic planar Hall effect. The quantum geometric nature of the planar Hall and nonlinear transport in altermagnets with the in-plane magnetic fields manifest itself as the conductivity σ^{xy} and $\sigma^{\alpha\beta;\gamma}$, which incorporates the intrinsic features of Bloch wave functions.

General theory of magnetotransport induced by quantum geometry —To begin with, we consider the target

		Planar Altermagnet		
		D wave	G wave	I wave
Longitudinal	QMSD (τ^0)	B^1	B^1	B^1
Transverse	BCSD (τ^1)	B^1	B^3	B^5
	QMSD (τ^0)	B^1	B^1	B^1
	BCS (τ^0)	B^2	B^4	B^6

FIG. 2. Comparison between the responses in different C_nT symmetry of planar altermagnets coupled with planar magnetic field. The scaling behavior with respect to magnetic field depends on different altermagnetic order parameters.

model Hamiltonian $H = H_0 + H_B$ with H_0 describing the bare system of our interest and H_B denoting the Zeeman energy $H_B = -g_s\mu_B B \hat{S}$ induced by an in-plane magnetic field B , where g_s is the Landré-g factor, μ_B is the Bohr magneton and \hat{S} is the spin operator of electron. Concretely, quantum metric and Berry curvature are defined as the real symmetric and imaginary antisymmetric parts of the quantum geometric tensor, namely $Q_{ab}^n = \text{tr}(P^n \partial_a P^n \partial_b P^n) = g_{ab}^n - \frac{i}{2}\Omega_{ab}^n$, where P is a band projector in total Hamiltonian H and the trace is over internal degrees of freedom [32, 33].

We start by sketching the derivation of the linear and nonlinear conductivity, which takes the form $j^b = \sigma^{ab}E^a$ and $j^c = \sigma^{abc}E^aE^b$. The linear Hall conductivity is given by

$$\sigma^{xy} = \frac{e^2}{\hbar} \left(\int \frac{d\mathbf{k}}{(2\pi)^2} \sum_n \Omega_n^{xy} f_n \right), \quad (1)$$

and the second-order nonlinear conductivity is given by [15, 16]

$$\begin{aligned} \sigma^{ab;c} &= \frac{e^3 \tau}{\hbar^2} \sum_n \int_{\mathbf{k}} \frac{f_n}{2} (\partial_{k^a} \Omega_n^{bc} + \partial_{k^b} \Omega_n^{ac}) \\ &\quad - \frac{e^3}{\hbar} \sum_n \int_{\mathbf{k}} f_n \left[2\partial_{k^c} \tilde{g}_n^{ab} - \frac{1}{2} (\partial_{k^a} \tilde{g}_n^{bc} + \partial_{k^b} \tilde{g}_n^{ac}) \right], \end{aligned} \quad (2)$$

where Ω is the Berry curvature and \tilde{g} is the band-normalized quantum metric and f_n is the fermi distribution.

In altermagnets, due to the breaking of mirror and C_{2z} symmetries by the in-plane magnetic field, the magneto-transport properties governed by the quantum geometry can manifest. We can find how the quantum geometric quantities respond to the B field, i.e., expanding the quantum geometric quantities with respect to B . We consider the m -th order susceptibility with respect to the magnetic field of linear Hall conductivity $\sigma^{xy} = \kappa^{xy(m)} B^m$, as well as nonlinear conductivity

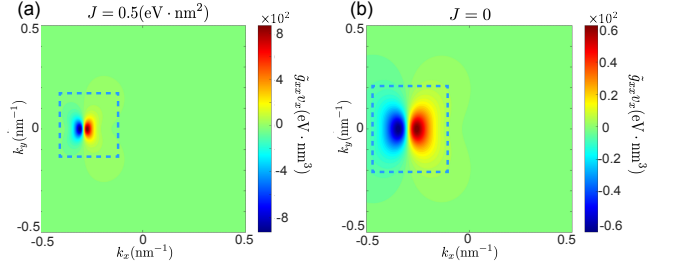


FIG. 3. Band-normalized quantum metric component multiplied by group velocity $\tilde{g}_{xx}v_x$ of d_{xy} planar altermagnet with different altermagnetic order magnitude: (a) $J = 0.5\text{eV}\cdot\text{nm}^2$; (b) $J = 0$. Other parameters are $v_R = 1\text{eV}\cdot\text{nm}$, $g_s\mu_B B = 0.2\text{eV}$.

$\sigma^{ab;c} = \chi^{ab;c(m)} B^m$. Importantly, κ and χ are instinct m -th order susceptibilities contributed by quantum geometry. Therefore, we define the quantum geometric tensor susceptibility as follows

$$\alpha_n^{bc(m)} = \partial_B^m \Omega_n^{bc} = 2 \text{Im} [\partial_B^m Q_n^{bc}] \Big|_{B \rightarrow 0}, \quad (3)$$

$$G_n^{bc(m)} = \partial_B^m \tilde{g}_n^{bc} = \text{Re} \left[\partial_B^m \frac{Q_n^{bc}}{\varepsilon_m - \varepsilon_n} \right] \Big|_{B \rightarrow 0}, \quad (4)$$

where α_n^{bc} and G_n^{bc} is the Berry curvature susceptibility and the band-normalized quantum metric susceptibility defined in both the crystal momentum k and the parameter B . Here, we derive the band-normalized quantum metric susceptibility

$$\begin{aligned} G_n^{bc(1)}(\mathbf{k}) &= \text{Re} \sum_{m \neq n} \left[\frac{3(S_{mm} - S_{nn}) v_{nm}^a v_{mn}^b}{(\varepsilon_m - \varepsilon_n)^4} \right. \\ &\quad + \sum_{l \neq m} \frac{S_{lm} v_{nl}^a v_{mn}^b + S_{lm}^* v_{nm}^a v_{ln}^b}{(\varepsilon_m - \varepsilon_n)^3 (\varepsilon_m - \varepsilon_l)} \\ &\quad \left. + \sum_{l \neq n} \frac{S_{ln}^* v_{lm}^a v_{mn}^b + S_{ln} v_{nm}^a v_{ml}^b}{(\varepsilon_m - \varepsilon_n)^3 (\varepsilon_n - \varepsilon_l)} \right]. \end{aligned} \quad (5)$$

Here $G_n^{bc(1)} = \text{Re} \left[\partial_B \frac{Q_n^{bc}}{\varepsilon_m - \varepsilon_n} \right] \Big|_{B \rightarrow 0}$ with $S_{nm} = -g_s\mu_B \langle u_n(\mathbf{k}) | \hat{S} | u_m(\mathbf{k}) \rangle$, $| u_m(\mathbf{k}) \rangle$ is the Bloch eigenstate of H_0 , $v_{x(y)}^{nm} = \langle u_n(\mathbf{k}) | \frac{\partial H}{\partial k_{x(y)}} | u_m(\mathbf{k}) \rangle$ is the velocity matrix element [34, 35].

In the following sections, we will examine how the nonlinear and nonreciprocal magnetotransport connects to the quantum geometric susceptibilities intrinsically. Note that throughout our work we do not study the high order extrinsic transport by the scattering time τ , which can be distinguished by the scaling analysis in experiments [15, 17].

Intrinsic Non-Reciprocal and Non Linear Hall Effect Induced by Quantum Geometry —To illustrate the features of the effect and the underlying geometric quantities, we first apply our theory to an effective Hamiltonian up to k^2 of a two-dimensional electron system with

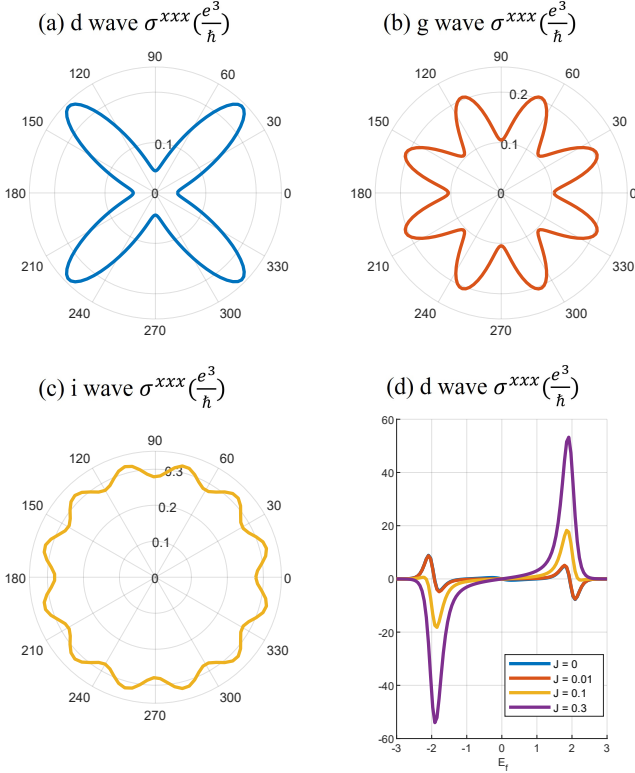


FIG. 4. The nonreciprocal longitudinal conductivity $\sigma^{x;xx} = \chi^{x;xx}|B|$ for d-, g-, and i-wave altermagnets. (a), (b) and (c) are the angular dependence of $\sigma^{x;xx}$; (d) The Fermi energy E_F dependence of $\sigma^{x;xx}$. Parameters: $J_d = J_g = J_i = 1$, $v_R = 1$, $T = 0.1$ (on unit of μ).

Rashba spin-orbit coupling and altermagnetic order parameter. The model reads:

$$\hat{H} = \frac{\mathbf{k}^2}{2m} + \hat{H}_s - \mu, \quad (6)$$

where μ is the chemical potential and \hat{H}_s is the spin part of the Hamiltonian given by

$$\hat{H}_s = \Delta_{\mathbf{k}}(\alpha)\sigma_z + v_R(\sigma_x k_y - \sigma_y k_x) - \mathbf{h} \cdot \boldsymbol{\sigma}, \quad (7)$$

where $\Delta_{\mathbf{k}}(\alpha)\sigma_z$ is the altermagnetic order parameter with the angular α characterizing the crystalline angle of planar altermagnets, $\mathbf{h} \cdot \boldsymbol{\sigma} = g_s\mu_B B \cos(\theta)\sigma_x + g_s\mu_B B \sin(\theta)\sigma_y$ is the Zeeman type of spin splitting [36]. Besides, the impact of the in-plane magnetic field on the altermagnet can be safely ignored due to the large altermagnetic spin splitting ($\sim 0.5\text{eV}$ [37]). For example, the saturation of the magnetization in the altermagnets RuO₂ and MnTe requires high magnetic fields up to 0.2 T [37–39]. To be specific, we consider typical altermagnetism as

$$\Delta_{\mathbf{k}}(\alpha) = \begin{cases} k'_x k'_y & (\text{d-wave}) \\ k'_x k'_y (k'^2_x - k'^2_y) & (\text{g-wave}) \\ k'_x k'_y (k'^2_x - 3k'^2_y)(3k'^2_x - k'^2_y) & (\text{i-wave}), \end{cases} \quad (8)$$

, where $k'_x = k_x \cos(\alpha) + k_y \sin(\alpha)$ and $k'_y = k_y \cos(\alpha) - k_x \sin(\alpha)$. We focus on specific material examples for different wave symmetries: d-wave altermagnets, such as Rb-doped V₂Te₂O and K-doped V₂Se₂O [40, 41]. For the g- and i-wave case, potential candidates are expected to be realized via external fields or chemical doping [42].

The generic second-order conductivity can be defined as $j^c = \sigma^{ab;c}(\mathbf{B})E^aE^b$, which is symmetric for the last two indices. Under global C_{2z} rotation, j and E change sign, so the conductance should also change sign. Meanwhile, the material remains the same due to its C_{2z} symmetry, so $\sigma^{ab;c}(-\mathbf{B}) = -\sigma^{ab;c}(\mathbf{B})$, namely the second-order conductivity must be an odd function of B . Hence, the $\mathbf{I} \cdot \mathbf{B}$ term is allowed in the conductivity tensor, which leads to anisotropic transport. Specifically, anisotropy transport is the current response $J \propto BE^2$ and is described by the conductivity σ that depends on the current \mathbf{I} and the external magnetic field \mathbf{B} as [13]

$$\sigma = \sigma_0 + \chi^{xx;x(1)} \mathbf{I} \cdot \mathbf{B}, \quad (9)$$

where σ_0 is the normal longitude conductivity induced by the Drude weight. In particular, $\chi^{xx;x}$ is the second-order longitudinal conductivity induced by the quantum metric susceptibility, which reads

$$\chi^{xx;x(1)} = -\frac{e^3}{\hbar} \sum_n \int_k \left(\partial_{k^x} G_n^{xx(1)}(\mathbf{k}) f_n + \partial_B f_n \tilde{g}_n^{xx} \right), \quad (10)$$

where $G_n^{xx(1)}(\mathbf{k})$ is first order quantum metric susceptibility defined in Eq. (4), B is the planar magnetic field, f_n is the fermion distribution.

Crucially, systems with Rashba SOC also exhibit an intrinsic contribution to $\chi^{xx;x}$ [3]. Consequently, neither the magnetic-field scaling (linear in $|B|$) nor the θ -periodicity (where θ is the polar angle of \mathbf{B}) of the nonreciprocal longitudinal conductivity can diagnose the $C_n\mathcal{T}$ symmetry, as both features are shared with the Rashba case. In Fig. 3 we plot the momentum-distribution of band-normalized quantum metric component multiplied by group velocity $\tilde{g}_{xx}v_x$ using the continuum model. It is clear that the altermagnetic order strongly enhance the quantity $\tilde{g}_{xx}v_x$, resulting in the giant nonreciprocal longitudinal transport in altermagnets, as we will see later. Detailed calculations demonstrating this are provided in the Supplementary Material [43].

However, the $C_n\mathcal{T}$ symmetry generates an anisotropic quantum metric susceptibility dipole. The dependence of this dipole on the in-plane altermagnet orientation α provides a clear diagnostic, as it differs distinctly among d-, g-, and i-wave orders, as shown in Fig. 4. Specifically, the response $\sigma^{x;xx} = \chi^{x;xx}|B|$ for d-, g-, and i-wave altermagnets exhibits different periodicities in α , a key distinction we demonstrate numerically for the d_{xy} , $g_{xy(x^2-y^2)}$, and $i_{xy(x^2-3y^2)(3x^2-y^2)}$ waves in Fig. 4. Notably, we find that the altermagnetic order strongly enhances the nonreciprocal conductivity compared to a system with pure

Rashba SOC, as shown in Fig. 4(d). And the value of the quantum metric also increases significantly in the case of alternating order, as shown in Fig. 3. These enhancements occur because the altermagnetic order reduces the energy gap, which strongly amplifies the quantum geometric effects. (see SM [43] for a detailed discussion.)

Without loss of generality, we calculate the second-order transverse conductivity as $j^y = \chi^{xx;y(m)} B^m E_x^2$. Unlike the longitudinal nonlinear conductivity, the transverse transport has two components that come from BCSD (extrinsic) and QMSD (intrinsic) and we focus on the nonlinear Hall effect contributed from the intrinsic contribution QMSD in this section.

$$\begin{aligned} \chi^{aa;b(1)} &= -\frac{e^3}{\hbar} \sum_n \int_k [(2\partial_{k^b} G_n^{aa(1)} - \partial_{k^a} G_n^{ab(1)}) f_n \\ &\quad + \partial_B f_n (2\partial_{k^b} \tilde{g}_n^{aa} - \partial_{k^a} \tilde{g}_n^{ab})] \end{aligned} \quad (11)$$

, where e is the electron, $G_n^{ab(1)}$ is the quantum metric susceptibility, and f_n is the fermion distribution. The scaling behavior and the θ angular periodicity of $\chi^{aa;b}$ are similar to $\chi^{xx;x}$ (longitudinal). (see SM [43] for a detailed discussion.)

Planar Hall Effect —The magnetic field induced Hall effect is given by the integral over the Berry curvature susceptibility in Eq. (3). The C_{2z} symmetry leads to $\sigma^{xy}(-B) = \sigma^{xy}(B)$. Therefore, we expect the leading order of linear Hall conductivity to be even in B , which does not conflict with the Onsager relation due to the even-parity magnetic order (The details can be found in the SM[43]). To further probe the magnetic symmetry of altermagnets, we examine the linear Hall conductivity, given by

$$\begin{aligned} \kappa^{xy(m)} &= \frac{e^2}{\hbar} \int \frac{d\mathbf{k}}{(2\pi)^2} \sum_n [\alpha_n^{xy(m)} f_n \\ &\quad + (\partial_B^m f_n) \Omega_n^{xy}] \end{aligned} \quad (12)$$

where $\alpha_n^{xy(m)}$ is the m -th order BCS and Ω_n^{xy} is the Berry curvature. The results of the linear Hall conductivity $\sigma^{xy}(B, \theta)$ of the d_{xy} , $g_{xy(x^2-y^2)}$, and $i_{xy(x^2-3y^2)(3x^2-y^2)}$ waves are shown in Fig. 5. We find that the number of zeros in θ , the periodicity in θ , and the leading order in B are different for these waves, indicating that the order of $\alpha_n^{xy(m)}$ defined in Eq. (3) are different for these waves. For d_{xy} , $g_{xy(x^2-y^2)}$ and $i_{xy(x^2-3y^2)(3x^2-y^2)}$, m are 2, 4 and 6, respectively.

To understand the angular dependence and the zero-crossings on the linear Hall conductivity, we analyze the symmetry constraints of the system. In the zero-field limit, the system characterized by $C_{2n}\mathcal{T}$ order parameter possesses a C_n symmetry. Crucially, the presence of a mirror symmetry M_y in our model, combined with the C_n symmetry, implies the existence of n vertical mirror

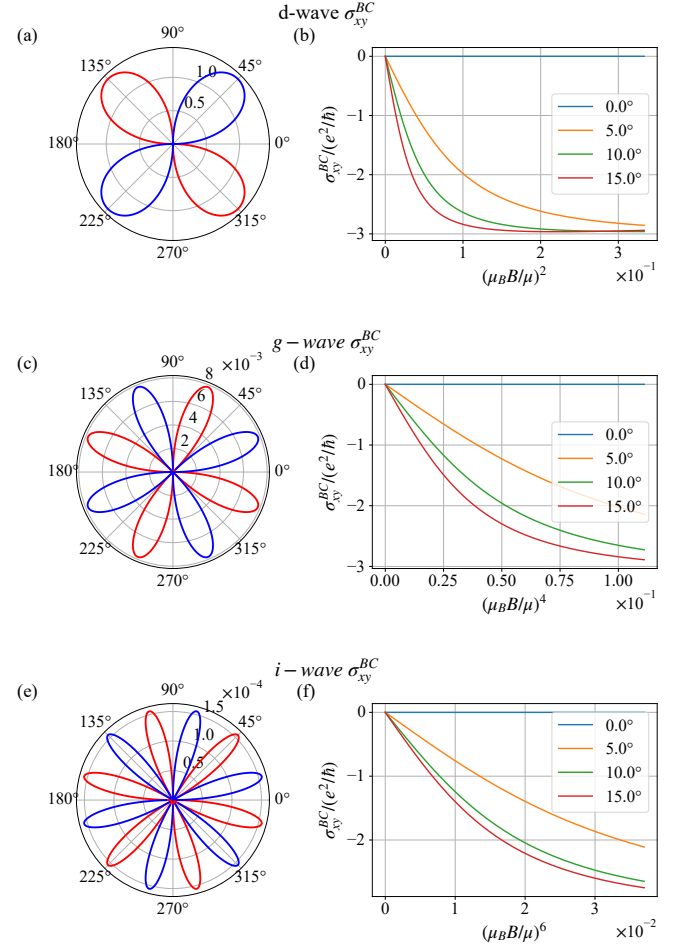


FIG. 5. The linear Hall conductivity of d -, g -, i -wave alternately magnetized systems. (a), (c) and (e) The angular dependence of Hall conductivity; (b), (d) and (f) The magnitude dependence of Hall conductivity at different directions. The parameters, in unit of μ , are $J_d = J_g = J_i = 1$, $v_R = 1$, $T = 0.1$.

planes in total that prohibit any linear Hall response. Applying an in-plane magnetic field generally breaks these symmetries, thereby inducing a finite planar Hall effect. However, if \mathbf{B} aligns perpendicularly to any of the mirror planes, the corresponding mirror symmetry remains preserved, strictly zeroing the Hall response. As a result, $\sigma^{xy}(B, \theta)$ vanishes whenever \mathbf{B} is normal to a mirror plane, imposing a periodicity of $\frac{2\pi}{n}$ on the angular dependence. Accordingly, the conductivity can be expanded as

$$\begin{aligned} \sigma^{xy(n)}(B, \theta) &= \sum_{l=1}^{\infty} B^{nl} C_l \sin(nl\theta + \phi_l) \\ &\approx B^n \kappa^{xy(n)}. \end{aligned} \quad (13)$$

Here $\phi_l = 0$ for our case. Keeping to the lowest order, we get the last line.

Nonlinear Planer Hall Effect. —The second-order conductivity $\sigma^{xx;y}$ is an odd function of B . In particular, the external second-order Hall response is induced

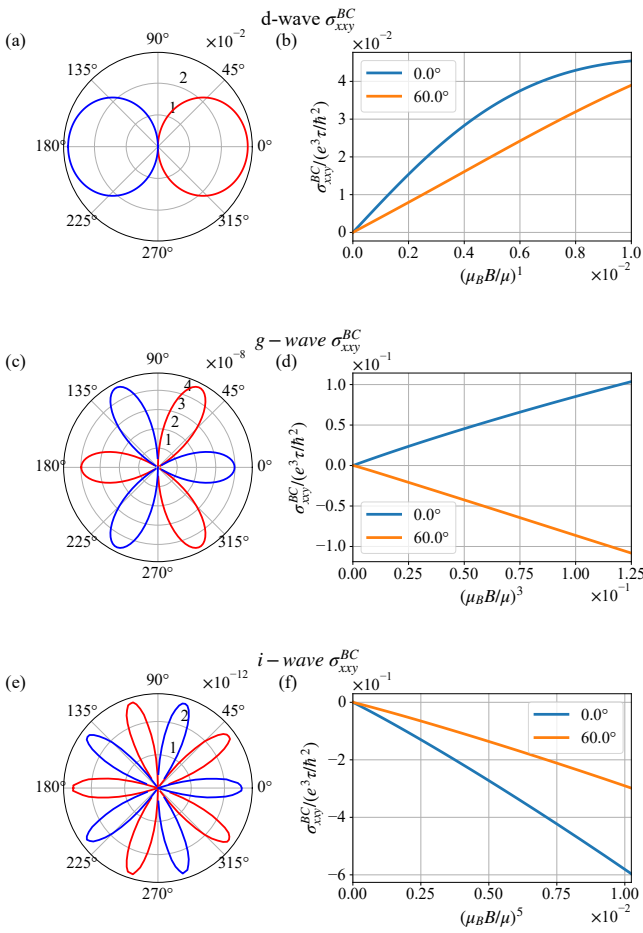


FIG. 6. BCSD-induced 2nd-order Hall conductivity $\sigma_{xx;y}^{BC}$ of d -, g -, i -wave altermagnets. (a), (c) and (e) are the angular dependence of $\sigma_{xx;y}^{BC}$ of d -, g -, i -wave altermagnets at $\mu_B B/\mu = 0.004$. (b), (d) and (f) are the magnitude dependence of $\sigma_{xx;y}^{BC}$ at different directions. $\sigma_{xx;y}^{BC}$ is in unit of $e^3\tau/\hbar^2$. The parameters, in unit of μ , are $J_d = J_g = J_i = 1$, $v_R = 1$, $T = 0.1$.

by the high-order Berry curvature susceptibility dipole

$$\chi^{aa;b(m)} = \frac{e^3\tau}{\hbar^2} \sum_n \int_k [\partial_{k^a} \alpha_n^{(m)ab} f_n + (\partial_B^m f_n) \partial_{k^a} \Omega^{ab}], \quad (14)$$

where τ is the scattering time and $\alpha_n^{(m)}$ is m-th order Berry curvature susceptibility.

The numerical results of BCSD induced second-order nonlinear planar Hall conductivity $\sigma_{xx;y}^{(m)} = \chi_{xx;y}^{(m)} |B|^m$ are shown in Fig. 6. The scaling behavior of the leading order in B again varies for different altermagnetic orders: $m = 1, 3, 5$, for d -, g -, i -wave, respectively. The $(n - 1)$ -fold symmetry of $\sigma_{xx;y}^{(m)}$ for the $C_{2n}T$ -altermagnet can be understood by the angular conservation argument. (For the detailed proof, see the Supplementary[43]).

Conclusion and Discussion —In summary, we have established a symmetry-based framework to quantify the band quantum geometry and magnetic geometry in altermagnets via planar magnetotransport. Regardless the specific model parameters, the general result is present in Fig. 2. At zero field, \mathcal{PT} -symmetric antiferromagnets forbid the Berry curvature dipole contribution to the nonlinear Hall effect, while the quantum metric dipole term remains allowed. In contrast, altermagnets with emergent C_{2z} or mirror symmetries forbid both contributions. An applied Zeeman field lifts these symmetry prohibitions and triggers quantum-geometry-governed responses. Specifically, the linear Hall conductivity arises from the BCS, the nonlinear Hall conductivity receives contributions from both the BCSD and QMSD, and the intrinsic nonreciprocal longitudinal transport stems solely from the QMSD.

Owing to the distinctive magnetic geometry of altermagnets, the nonreciprocal longitudinal response is governed by the anisotropic QMSD. In contrast, the linear and second-order Hall responses exhibit different magnetic-field scaling and distinct n -fold angular periodicities with respect to the in-plane field orientation, which vary for different altermagnetic orders. Furthermore, the anisotropic QMSD is strongly enhanced by the altermagnetic order compared to systems with SOC. These symmetry-dictated scalings and anisotropic effects enable the direct experimental discrimination of quantum geometry and provide a quantitative means to diagnose altermagnetic geometry.

* These authors contributed equally.

† zsunaw@connect.ust.hk

‡ jhuphy@ust.hk

- [1] S. Sankar, R. Liu, C.-P. Zhang, Q.-F. Li, C. Chen, X.-J. Gao, J. Zheng, Y.-H. Lin, K. Qian, R.-P. Yu, X. Zhang, Z. Y. Meng, K. T. Law, Q. Shao, and B. Jäck, Experimental evidence for a berry curvature quadrupole in an antiferromagnet, *Phys. Rev. X* **14**, 021046 (2024).
- [2] J.-X. Hu, Z.-T. Sun, Y.-M. Xie, and K. T. Law, Josephson diode effect induced by valley polarization in twisted bilayer graphene, *Phys. Rev. Lett.* **130**, 266003 (2023).
- [3] G. Sala, M. T. Mercaldo, K. Domi, S. Gariglio, M. Cuoco, C. Ortix, and A. D. Caviglia, The quantum metric of electrons with spin-momentum locking, *Science* **389**, 822 (2025), <https://www.science.org/doi/pdf/10.1126/science.adq3255>.
- [4] J.-X. Hu, S. A. Chen, and K. T. Law, Geometric and conventional contributions of superconducting diode effect: Application to flat-band systems, *Phys. Rev. B* **111**, 174513 (2025).
- [5] C.-P. Zhang, J. Xiao, B. T. Zhou, J.-X. Hu, Y.-M. Xie, B. Yan, and K. T. Law, Giant nonlinear hall effect in strained twisted bilayer graphene, *Phys. Rev. B* **106**, L041111 (2022).
- [6] J.-X. Hu, O. Matsyshyn, and J. C. W. Song, Nonlinear

- superconducting magnetoelectric effect, *Phys. Rev. Lett.* **134**, 026001 (2025).
- [7] J.-X. Hu, C. Zeng, and Y. Yao, Colossal layer nernst effect in twisted moiré layers, *Phys. Rev. B* **109**, L201403 (2024).
- [8] C. Tzschaschel, J.-X. Qiu, X.-J. Gao, H.-C. Li, C. Guo, H.-Y. Yang, C.-P. Zhang, Y.-M. Xie, Y.-F. Liu, A. Gao, D. Bérubé, T. Dinh, S.-C. Ho, Y. Fang, F. Huang, J. Nordlander, Q. Ma, F. Tafti, P. J. W. Moll, K. T. Law, and S.-Y. Xu, Nonlinear optical diode effect in a magnetic weyl semimetal, *Nature Communications* **15**, 3017 (2024).
- [9] Z. Wu, B. T. Zhou, X. Cai, P. Cheung, G.-B. Liu, M. Huang, J. Lin, T. Han, L. An, Y. Wang, S. Xu, G. Long, C. Cheng, K. T. Law, F. Zhang, and N. Wang, Intrinsic valley hall transport in atomically thin mos₂, *Nature Communications* **10**, 611 (2019).
- [10] I. Sodemann and L. Fu, Quantum nonlinear hall effect induced by berry curvature dipole in time-reversal invariant materials, *Phys. Rev. Lett.* **115**, 216806 (2015).
- [11] C.-P. Zhang, X.-J. Gao, Y.-M. Xie, H. C. Po, and K. T. Law, Higher-order nonlinear anomalous hall effects induced by berry curvature multipoles, *Phys. Rev. B* **107**, 115142 (2023).
- [12] X. F. Lu, C.-P. Zhang, N. Wang, D. Zhao, X. Zhou, W. Gao, X. H. Chen, K. T. Law, and K. P. Loh, Nonlinear transport and radio frequency rectification in bitebr at room temperature, *Nature Communications* **15**, 245 (2024).
- [13] T. Morimoto and N. Nagaosa, Chiral anomaly and giant magnetochiral anisotropy in noncentrosymmetric weyl semimetals, *Phys. Rev. Lett.* **117**, 146603 (2016).
- [14] Y. Tokura and N. Nagaosa, Nonreciprocal responses from non-centrosymmetric quantum materials, *Nature Communications* **9**, 3740 (2018).
- [15] N. Wang, D. Kaplan, Z. Zhang, T. Holder, N. Cao, A. Wang, X. Zhou, F. Zhou, Z. Jiang, C. Zhang, S. Ru, H. Cai, K. Watanabe, T. Taniguchi, B. Yan, and W. Gao, Quantum-metric-induced nonlinear transport in a topological antiferromagnet, *Nature* **621**, 487 (2023).
- [16] D. Kaplan, T. Holder, and B. Yan, Unification of nonlinear anomalous hall effect and nonreciprocal magnetoresistance in metals by the quantum geometry, *Phys. Rev. Lett.* **132**, 026301 (2024).
- [17] H. Li, C. Zhang, C. Zhou, C. Ma, X. Lei, Z. Jin, H. He, B. Li, K. T. Law, and J. Wang, Quantum geometry quadrupole-induced third-order nonlinear transport in antiferromagnetic topological insulator MnBi₂Te₄, *Nature Communications* **15**, 7779 (2024).
- [18] C. Wang, Y. Gao, and D. Xiao, Intrinsic nonlinear hall effect in antiferromagnetic tetragonal cumnas, *Phys. Rev. Lett.* **127**, 277201 (2021).
- [19] H. Liu, J. Zhao, Y.-X. Huang, W. Wu, X.-L. Sheng, C. Xiao, and S. A. Yang, Intrinsic second-order anomalous hall effect and its application in compensated antiferromagnets, *Phys. Rev. Lett.* **127**, 277202 (2021).
- [20] S. A. Chen and K. T. Law, Ginzburg-landau theory of flat-band superconductors with quantum metric, *Phys. Rev. Lett.* **132**, 026002 (2024).
- [21] J.-X. Hu, S. A. Chen, and K. T. Law, Anomalous coherence length in superconductors with quantum metric, *Communications Physics* **8**, 20 (2025).
- [22] Z. C. F. Li, Y. Deng, S. A. Chen, D. K. Efetov, and K. T. Law, Flat band josephson junctions with quantum metric, *Phys. Rev. Res.* **7**, 023273 (2025).
- [23] B. T. Zhou, V. Pathak, and M. Franz, Quantum-geometric origin of out-of-plane stacking ferroelectricity, *Phys. Rev. Lett.* **132**, 196801 (2024).
- [24] X. Guo, X. Ma, X. Ying, and K. T. Law, Majorana zero modes in the lieb-kitaev model with tunable quantum metric, *Phys. Rev. Lett.* **135**, 076601 (2025).
- [25] C. Song, H. Bai, Z. Zhou, L. Han, H. Reichlova, J. H. Dil, J. Liu, X. Chen, and F. Pan, Altermagnets as a new class of functional materials, *Nature Reviews Materials* **10**, 473 (2025).
- [26] L. Šmejkal, J. Sinova, and T. Jungwirth, Beyond conventional ferromagnetism and antiferromagnetism: A phase with nonrelativistic spin and crystal rotation symmetry, *Phys. Rev. X* **12**, 031042 (2022).
- [27] L. Šmejkal, J. Sinova, and T. Jungwirth, Emerging research landscape of altermagnetism, *Phys. Rev. X* **12**, 040501 (2022).
- [28] S. Sheoran and P. Dev, Spontaneous anomalous hall effect in two-dimensional altermagnets, *Phys. Rev. B* **111**, 184407 (2025).
- [29] Y. Fang, J. Cano, and S. A. A. Ghorashi, Quantum geometry induced nonlinear transport in altermagnets, *Phys. Rev. Lett.* **133**, 106701 (2024).
- [30] R. Y. Chu, L. Han, Z. H. Gong, X. Z. Fu, H. Bai, S. X. Liang, C. Chen, S.-W. Cheong, Y. Y. Zhang, J. W. Liu, Y. Y. Wang, F. Pan, H. Z. Lu, and C. Song, Third-order nonlinear hall effect in altermagnet ruo₂, *Phys. Rev. Lett.* **135**, 216703 (2025).
- [31] M. Roig, A. Kreisel, Y. Yu, B. M. Andersen, and D. F. Agterberg, Minimal models for altermagnetism, *Physical Review B* **110**, 144412 (2024).
- [32] Y. Jiang, T. Holder, and B. Yan, Revealing quantum geometry in nonlinear quantum materials, *Reports on Progress in Physics* **88**, 076502 (2025).
- [33] A. Gao, N. Nagaosa, N. Ni, and S.-Y. Xu, *Quantum geometry phenomena in condensed matter systems* (2025), arXiv:2508.00469 [cond-mat.str-el].
- [34] J.-X. Hu and J. C. W. Song, *Orbital longitudinal magneto-electric coupling in multilayer graphene* (2025), arXiv:2503.07822 [cond-mat.mes-hall].
- [35] C. Cui, R.-W. Zhang, Y. Qiu, Y. Han, Z.-M. Yu, and Y. Yao, Electric hall effect and quantum electric hall effect, *Physical Review Letters* **135**, 116301 (2025).
- [36] C.-X. Liu, X.-L. Qi, H. Zhang, X. Dai, Z. Fang, and S.-C. Zhang, Model hamiltonian for topological insulators, *Phys. Rev. B* **82**, 045122 (2010).
- [37] R. Chen, Z.-M. Wang, K. Wu, H.-P. Sun, B. Zhou, R. Wang, and D.-H. Xu, Probing *k*-space alternating spin polarization via the anomalous hall effect, *Phys. Rev. Lett.* **135**, 096602 (2025).
- [38] T. Tschirner, P. Keßler, R. D. Gonzalez Betancourt, T. Kotte, D. Kriegner, B. Büchner, J. Dufouleur, M. Kamp, V. Jovic, L. Smejkal, J. Sinova, R. Claessen, T. Jungwirth, S. Moser, H. Reichlova, and L. Veyrat, Saturation of the anomalous hall effect at high magnetic fields in altermagnetic ruo₂, *APL Materials* **11**, 101103 (2023), https://pubs.aip.org/aip/apm/article-pdf/doi/10.1063/5.0160335/18147898/101103_1.5.0160335.pdf.
- [39] R. D. Gonzalez Betancourt, J. Zubáč, R. Gonzalez-Hernandez, K. Geishendorf, Z. Šobáň, G. Springholz, K. Olejník, L. Šmejkal, J. Sinova, T. Jungwirth, S. T. B. Goennenwein, A. Thomas, H. Reichlová, J. Železný, and D. Kriegner, Spontaneous anomalous hall effect arising

- from an unconventional compensated magnetic phase in a semiconductor, *Phys. Rev. Lett.* **130**, 036702 (2023).
- [40] F. Zhang, X. Cheng, Z. Yin, C. Liu, L. Deng, Y. Qiao, Z. Shi, S. Zhang, J. Lin, Z. Liu, M. Ye, Y. Huang, X. Meng, C. Zhang, T. Okuda, K. Shimada, S. Cui, Y. Zhao, G.-H. Cao, S. Qiao, J. Liu, and C. Chen, *Crystal-symmetry-paired spin-valley locking in a layered room-temperature antiferromagnet* (2024), arXiv:2407.19555 [cond-mat.str-el].
- [41] B. Jiang, M. Hu, J. Bai, Z. Song, C. Mu, G. Qu, W. Li, W. Zhu, H. Pi, Z. Wei, Y.-J. Sun, Y. Huang, X. Zheng, Y. Peng, L. He, S. Li, J. Luo, Z. Li, G. Chen, H. Li, H. Weng, and T. Qian, A metallic room-temperature d-wave altermagnet, *Nature Physics* **21**, 754–759 (2025).
- [42] G. Yang, Z. Li, S. Yang, J. Li, H. Zheng, W. Zhu, Z. Pan, Y. Xu, S. Cao, W. Zhao, A. Jana, J. Zhang, M. Ye, Y. Song, L.-H. Hu, L. Yang, J. Fujii, I. Vobornik, M. Shi, H. Yuan, Y. Zhang, Y. Xu, and Y. Liu, Three-dimensional mapping of the altermagnetic spin splitting in crsb, *Nature Communications* **16**, 10.1038/s41467-025-56647-7 (2025).
- [43] See Supplemental Material for calculation methods and detailed analysis.